The FASEB Journal article fj.11-186197. Published online November 2, 2011.



# Misfolded proteins inhibit proliferation and promote stress-induced death in SV40-transformed mammalian cells

**Mehmet Alper Arslan, Maria Chikina,[1] Péter Csermely, and Csaba Sőti[2]**
Department of Medical Chemistry, Semmelweis University, Budapest, Hungary

ABSTRACT **Protein misfolding is implicated in neurodegenerative diseases and occurs in aging. However, the contribution of the misfolded ensembles to toxicity remains largely unknown. Here we introduce 2 primate cell models of destabilized proteins devoid of specific cellular functions and interactors, as *bona fide* misfolded proteins, allowing us to isolate the gain-of-function of non-native structures. Both GFP-degron and a mutant chloramphenicol-acetyltransferase fused to GFP (GFP-Δ9CAT) form perinuclear aggregates, are degraded by the proteasome, and colocalize with and induce the chaperone Hsp70 (HSPA1A/B) in COS-7 cells. We find that misfolded proteins neither significantly compromise chaperone-mediated folding capacity nor induce cell death. However, they do induce growth arrest in cells that are unable to degrade them and promote stress-induced death upon proteasome inhibition by MG-132 and heat shock. Finally, we show that overexpression of all heat-shock factor-1 (HSF1) and Hsp70 proteins, as well as wild-type and deacetylase-deficient (H363Y) SIRT1, rescue survival upon stress, implying a noncatalytic action of SIRT1 in response to protein misfolding. Our study establishes a novel model and extends our knowledge on the mechanism of the function-independent proteotoxicity of misfolded proteins in dividing cells.—Arslan, M. A., Chikina, M., Csermely, P., Sőti, C. Misfolded proteins inhibit proliferation and promote stress-induced death in SV40-transformed mammalian cells. *FASEB J.* 26, 000–000 (2012). www.fasebj.org**

*Key Words: HSF1 · Hsp70 · sirtuin*

Protein misfolding has been implicated in the etiology of neurodegenerative diseases and aging, although the molecular mechanisms remain elusive (1). Proteins may misfold due to inherent mutations (1), mistranslation (2), in response to denaturing stress, or from post-translational modifications (3–4) resulting in diverse non-native conformations. However, misfolding-induced exposure of hydrophobic surfaces generally results in incorrect protein-protein interactions, by which misfolded oligomeric species gain a cytotoxic function (5–6). These mechanisms are supported by studies using both repeat-expansion mutants linked to neurodegeneration and observations on non-disease-associated proteins (7–9). In these models, however, the loss of physiological function and misfolding-induced alterations in specific protein-protein interactions could not be ruled out. Hence, the exact contribution of misfolded ensembles, *per se*, to cytotoxicity is largely unclear.

Protein maintenance is achieved by a complex proteostasis network including molecular chaperones (10). Many chaperones are heat-shock proteins induced by proteotoxic stress *via* heat-shock factor-1 (HSF1; ref. 11). The heat-shock response is considered the prime sensor of misfolded proteins in the cytosol (12), suggesting that a common structural determinant of non-native ensembles mediates both their recognition and cytotoxicity. Indeed, chaperones confer protection by preventing misfolding, as well as by promoting clearance and sequestration of misfolded proteins into aggregates (13). The heat-shock response declines during aging, with a concomitant accumulation of protein aggregates, especially in postmitotic tissues (14–15). Moreover, both aging and chronic expression of polyQ expansions disrupt proteostasis in *Caenorhabditis elegans* (16–17). However, it is unknown how short-term expression of a single misfolded protein affects proteostasis in replicating cells.

Green fluorescent protein (GFP) and chloramphenicol-acetyltransferase (CAT) are widely used reporters in mammalian cells. A C-terminal fusion of a degron peptide to GFP has been reported to aggregate and induce cytotoxicity in *C. elegans* and in mammalian neurons (18), and a C-terminally truncated form of CAT (Δ9CAT) has been shown to form inclusion bodies in *Escherichia coli* (19). Both variants are almost identical to their wild-type counterparts in sequence, meaning no major difference in costs of their expression and degradation. They lack disease-associated se-

[1] Current address: Department of Neurology, Mt. Sinai School of Medicine, New York, NY, USA.
[2] Correspondence: Semmelweis University, Department of Medical Chemistry, Tüzoltó u. 37–47. Budapest, H-1094, Hungary. E-mail: csaba.soti@eok.sote.hu
doi: 10.1096/fj.11-186197
This article includes supplemental data. Please visit *http://www.fasebj.org* to obtain this information.

quences, high-affinity interactors, and cellular function, which eliminates mechanisms originating from sequence-specific interactions and from losing functional benefits upon misfolding. Hence, we introduce both mutants as *bona fide* misfolded proteins in COS-7 cells, allowing the isolation of the gains of function of misfolded ensembles. In this report, we analyze their turnover, effect on the heat-shock response, chaperone-mediated protein folding, cell proliferation, and survival under basal and stress conditions. Finally, we address how genetic up-regulation of major stress-inducible defense mechanisms combat the challenge induced by protein misfolding.

## MATERIALS AND METHODS

### Constructs

pEGFP-C1 was obtained from Clontech Laboratories (BD Biosciences, San Jose, CA, USA). GFP-degron was a kind gift of Christopher Link (University of Colorado, Boulder, CO, USA). GFP-wtCAT was generated by cloning the PCR-amplified full-length CAT (pCAT3-Control vector; Promega, Madison, WI, USA) region into the *BglII*/*PstI* sites of pEGFP-C1, using forward primer 5′-AAAGATCTATGGAGAAAAAAAT-CAC-3′ and reverse primer 5′-AACTGCAGTTACGCCCCGC-3′. For GFP-Δ9CAT cloning, the reverse primer was designed to omit sequences corresponding to the last 9 C-terminal amino acids (5′-AACTGCAGTTACTGTTGTAATTC-3′). Expression plasmids were kind gifts of the following colleagues: His-cBSA, Richard Voellmy (University of Miami, Miami, FL, USA); GFP170*, Elizabeth Sztul (University of Alabama, Birmingham, AL, USA); Hsp70.1pr-luc, Rick Morimoto (Northwestern University, Evanston, IL, USA); HSF1-myc-His, Lea Sistonen (Åbo Akademi University, Turku, Finland); Hsp70-myc, Kerstin Bellmann (Heinrich-Heine University, Düsseldorf, Germany); SIRT6-Flag, Haim Cohen (Bar-Ilan University, Ramat-Gan, Israel). Wild-type and deacetylase-deficient (H363Y) SIRT1 were obtained from Addgene (Cambridge, MA, USA). CMV-β-galactosidase was purchased from Promega, and pTK-luc was provided by László Hunyady (Semmelweis University, Budapest, Hungary). All constructs were verified by DNA sequencing.

### Cell culture and transfection

COS-7 cells (SV40-transformed African green monkey kidney fibroblast-like cell line; CRL-1651; American Type Culture Collection, Manassas, VA, USA) were cultured in Dulbecco's modified Eagle medium (with 4.5 mg/ml glucose; Life Technologies–Invitrogen, Carlsbad, CA, USA), supplemented with 10% fetal bovine serum, 100 U/ml penicillin and 100 μg/ml streptomycin, and 2 mM L-glutamine in a humidified incubator at 37°C with 5% $CO_2$. Cells were plated at a density of 2.8–3 × $10^4$ cells/$cm^2$, 1 d before transfection. Transient transfections were performed by Lipofectamine LTX reagent (Invitrogen) with the indicated plasmids according to the manufacturer's guidelines at a total DNA (μg) to Lipofectamine (μl) ratio of 1:3. Cells were processed for analyses at 24 or 48 h post-transfection.

### Purification of aggregates and Western blotting

Cells were lysed in 1% Triton X-100 in PBS with protease inhibitors (Complete; Roche, Mannheim, Germany) for 30 min at 4°C. After sonication on ice for 3 × 10 s, the lysates were cold-centrifuged (4°C) at 12,500 *g* for 15 min, and supernatants (S) containing soluble proteins were transferred to new tubes. Detergent-insoluble pellets (P), containing aggregated proteins, were solubilized in urea buffer (2% SDS, 6 M urea, 30 mM TrisHCl, pH 7.6) in the same volume, by shaking at 600 rpm for 10 min at 50°C. Equal volumes of protein extracts from each fraction (S, P) were resolved by SDS-PAGE. Western blotting was performed by transfer to nitrocellulose membrane (Bio-Rad, Hercules, CA) and by blocking in 5% (w/v) skim milk powder (Fluka, Buchs, Switzerland). Blots were probed with antibodies against GFP (20) and Hsp70 (HSPA1A/B; SPA-810; Stressgen, San Diego, CA), HSF1 (Cell Signaling, Danvers, MA, USA), SIRT1 (Cell Signaling), and SIRT6 (Sigma-Aldrich, St. Louis, MO, USA). Immunodetection was performed by ECL (PerkinElmer, Wellesley, MA, USA).

### Estimation of misfolded protein expression levels

Cells were trypsinized and split, and the ratio of $GFP^+$ cells was determined by flow cytometry (FACSCalibur; BD Biosciences, Heidelberg, Germany) using the FL1 (530/30 BP) channel. The rest of the cells were lysed in urea buffer, and protein concentration was determined by detergent-compatible BCA protein assay (Pierce, Rockford, IL, USA). Protein extracts (10 μg) were loaded on SDS-PAGE along with known quantities of recombinant GFP (Roche). GFP expression levels (% of total protein) were determined by densitometric analysis of the GFP Western blots using Image J (U.S. National Institutes of Health, Bethesda, MD, USA), normalized to the corresponding $GFP^+$ cell ratio.

### Immunofluorescence microscopy

Cells were grown on poly-L-lysine-coated (0.1 mg/ml; Sigma) glass coverslips. At 2 d after transfection, cells were fixed and permeabilized in prechilled (−20°C) absolute methanol for 5 min. After being washed twice in PBS, cells were blocked in 1% BSA, then incubated in an anti-Hsp70 mouse monoclonal antibody solution (BD Biosciences) recognizing both inducible (HSPA1A/B) and constitutive (HSPA8) Hsp70 for 1 h at room temperature. Following washing, cells were stained by Cy3-conjugated goat anti-mouse secondary antibody (Jackson ImmunoResearch Labs, West Grove, PA, USA) for 30 min at room temperature. After washing, cells were counterstained with DAPI (Molecular Probes, Eugene, OR, USA). Coverslips were mounted using Vectashield (Vector Laboratories, Burlingame, CA, USA) and visualized by epifluorescence microscope (Nikon Eclipse E400; Nikon, Tokyo, Japan), employing ×10 × 100 (oil immersion) power with the appropriate filter sets.

### HSF1 transactivation and luciferase folding assays

Cells were cotransfected with a reporter plasmid harboring the *hsp70* promoter region upstream of the firefly luciferase gene (hsp70.1pr-luc) and a β-galactosidase plasmid driven by the cytomegalovirus promoter (β-gal) for an internal control. For luciferase folding, a firefly luciferase plasmid harboring the thymidine kinase minimal promoter (TK-luc) was used. Cotransfections were done at a ratio of 4:1:1. Cells were lysed in 1X Reporter Lysis Buffer (Promega) for 20 min at room temperature with occasional rocking. For luciferase folding assay, cells were immediately cooled on ice to prevent renaturation of luciferase, and cell lysis was performed on an ice bed for 40 min. Then cells were centrifuged (4°C) at 12,500 *g* for 3 min. Cell lysates were processed for β-galactosidase

and luciferase (Bright-Glo; Promega) assays according to the manufacturer's protocols. Absorbances and luminescence were measured by a plate reader (Thermo Varioskan Flash; Thermo Scientific, Wiesbaden, Germany). Data were expressed by dividing luminescence values by β-gal activities (luc/β-gal).

### BrdU incorporation

Cells grown on poly-L-lysine-coated coverslips were pulse-labeled with bromodeoxyuridine (BrdU; Molecular Probes) at 100 μM for 3 h. After being washed once in PBS, cells were fixed in 4% paraformaldehyde (Sigma) at 4°C for 30 min. Following washing in PBS containing 0.5% (w/v) BSA (wash buffer), cells were permeabilized in 1% Triton-X in PBS for 20 min at room temperature, then stained with FITC-conjugated anti-GFP antibody (Abcam, Cambridge, MA, USA) for 40 min at room temperature. Following washing, genomic DNA was denatured in 2 M HCl containing 0.5% Tween-20 for 30 min at 37°C. Cells were stained with Alexa Fluor 546-conjugated anti-BrdU antibody (Molecular Probes) for 40 min at room temperature. Following multiple washes, cells were counterstained with DAPI for 5 min and analyzed by an epifluorescence microscope (DMI6000B; Leica Microsystems, Wetzlar, Germany), employing ×10 × 10 power with the appropriate filter sets (DAPI: A4, FITC: L5, Alexa Fluor 546: TX2). Image analysis was performed by counting 600–700 cells/ area for 6 different areas randomly selected from each sample.

### Annexin assay

Cells were treated with the proteasome inhibitor MG-132 (2 μM; Calbiochem, San Diego, CA, USA) on the same day of transfection, for a total duration of 42 h. Cells were trypsinized and cold-centrifuged (4°C) at 2000 rpm for 5 min. Following washing in ice-cold PBS, cells were resuspended in 100 μl annexin buffer (10 mM HEPES, 140 mM NaCl, and 2.5 mM $CaCl_2$) and stained with 5 μl annexin V-Alexa Fluor 647 conjugate (Molecular Probes–Invitrogen) for 20 min at room temperature. After the addition of 900 μl annexin buffer, cells were mixed gently and immediately analyzed by flow cytometry. Cells were counted (10,000) and gated in an FSC/SSC dot plot to eliminate cell debris. Acquisition and analysis were done by BD CellQuest Pro software (BD Biosciences). Native GFP and annexin signals were measured in a dual-parameter dot plot by FL1 (530/30 BP) *vs.* FL4 (661/16 BP) channels, respectively. The percentage of annexin$^+$ cells out of the GFP$^+$ subpopulation was calculated by the formula UR/(UR+LR)×100, as obtained from quadrant statistics.

### Analysis of cellular DNA content

Cells were treated with 2 μM MG-132 1 day after transfection for 20 h. For concomitant heat-stress experiments, cells were heat-shocked at 43°C or kept 37°C at for 30 min in a circulating water bath. Cells were collected and cold-centrifuged (4°C) at 1800 rpm for 3 min. The resulting cell pellet was resuspended in 1 ml prechilled (at −20°C) 70% ethanol at room temperature for 30 min, then stored at −20°C overnight. Fixed cells were pelleted at 2200 rpm for 5 min at 4°C and resuspended in 1 ml extraction buffer (200 mM $Na_2HPO_4$, pH 7.8, adjusted with 200 mM citric acid) containing 10 μg/ml final concentration of RNase A (Sigma). Following incubation at room temperature for 30 min, the remaining nuclear DNA was stained by propidium iodide (10 μg/ml) for 10 min at room temperature. Gated total cell population was immediately analyzed by a flow cytometer (FACSCalibur; BD Biosciences) in a 2-parameter dot plot with FL1 (530/30 BP) *vs.* FL3 (650 LP) channels, measuring the native GFP and PI fluorescence, respectively. For data analysis (BD CellQuest Pro), only the percentage of GFP$^+$ cells with an intact cell cycle (*i.e.*, combination of $G_1$-S-$G_2$/M peaks) out of the gated total population (*i.e.*, UR values obtained from the quadrant statistics) was taken into consideration.

### Statistical analysis

Data were analyzed using SPSS 15.0 software (SPSS, Chicago, IL, USA) and compared by Student's *t* test. All data are presented as means ± SE of indicated numbers of independent experiments. Values of $P < 0.05$ were considered significant.

## RESULTS

### GFP-degron and GFP-Δ9CAT display characteristics of misfolding

First, we generated GFP-fusions of wild-type (wtCAT) and Δ9CAT and used GFP and GFP-degron and CAT variants to transiently transfect COS-7 cells and investigated their solubility by sequential extraction into detergent-soluble and insoluble fractions. While GFP and GFP-wtCAT showed an equal distribution, GFP-degron and GFP-Δ9CAT sedimented predominantly in detergent-insoluble pellet fractions, respectively (**Fig. 1*A***). This sedimentation was not due to higher-level overexpression, since both mutants were detected at a level 2- to 5-fold less than their wild-type counterparts (see the sum of S+P fractions in Figs. 1*A* and **2*A***). Moreover, we observed GFP-reactive bands at higher molecular weight in the pellet fractions of GFP-degron and GFP-Δ9CAT, indicating the presence of insoluble oligomeric and/or ubiquitinylated species, both of which indicate the exposure of buried regions in misfolded ensembles. Spectrophotometric CAT assays (21) revealed that deletion of the 9 C-terminal amino acids also caused total loss of CAT enzymatic activity (Supplemental Fig. S1). Thus, destabilizing modifications induced the loss of native conformation and converted both GFP and GFP-wtCAT into a less soluble state.

Next, we examined the subcellular distribution of GFP-degron and GFP-Δ9CAT by fluorescence microscopy. Both GFP-degron and GFP-Δ9CAT prevailed predominantly as deposits of perinuclear aggregates resembling aggresomes, while GFP and GFP-wtCAT distributed diffusely (Fig. 1*B*). These observations have been confirmed in live cells (data not shown) and demonstrated that the decreased solubility was not an artifact caused by cell lysis, but was due to the formation of aggregated ensembles inside living cells, a hallmark of protein misfolding (3). Our findings on the perinuclear deposition of GFP-degron are consistent with those of Link *et al.* (18).

Expression of both GFP-degron and GFP-Δ9CAT increased the level of inducible Hsp70 (HSPA1A/B; Fig. 1*A*, bottom panel). Equally increased Hsp70 levels were observed in the soluble and pellet fractions,

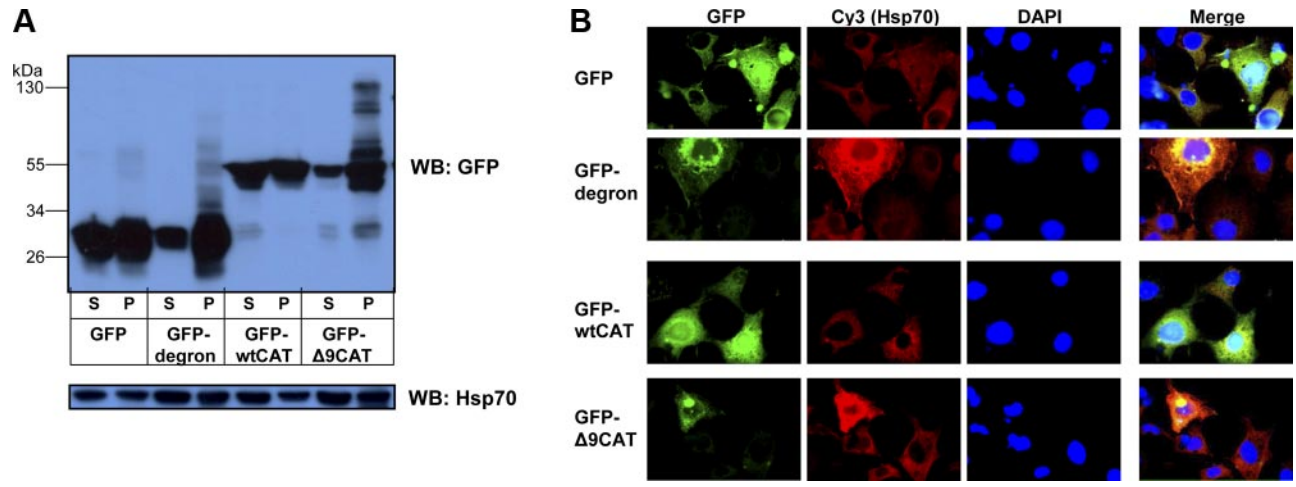


**Figure 1.** GFP-degron and GFP-Δ9CAT display characteristics of misfolding. *A*) Misfolding GFP-degron and GFP-Δ9CAT proteins sediment in detergent-insoluble aggregates and increase Hsp70 (HSPA1A/B) protein level. After transient transfections with the indicated constructs (GFP, GFP-degron, GFP-wtCAT, GFP-Δ9CAT), COS-7 cells were lysed, and cell lysates were separated into soluble (S) and detergent-insoluble pellet (P) fractions by centrifugation and analyzed by Western blotting for GFP and Hsp70, respectively. *B*) Misfolding proteins form perinuclear aggregates and accumulate total Hsp70 protein *in vivo*. Transfected cells grown on coverslips were fixed in methanol; stained by an antibody recognizing both inducible (HSPA1A/B) and constitutive (HSPA8) Hsp70, followed by a Cy3-conjugated secondary antibody, and DAPI for nuclear DNA; and were visualized under a fluorescence microscope. Images are representatives of 5 independent experiments.

respectively, of both mutants, indicating that Hsp70 did not show a strong preference toward insoluble species after cell lysis. Moreover, immunofluorescence analyses showed that GFP-degron and GFP-Δ9CAT led to a robust constitutive and inducible Hsp70 (HSPA8 and HSPA1A/B, respectively) accumulation only in cells where they were expressed, in contrast to the soluble controls GFP and GFP-wtCAT (Fig. 1*B*). Remarkably, Hsp70 was strongly enriched in both GFP-degron and GFP-Δ9CAT aggregates. The Western blot and immunofluorescence data together suggest a transient association of Hsp70 with the misfolded/aggregated species of GFP-degron and GFP-Δ9CAT and are consistent with a previous report showing a dynamic interaction of Hsp70 with polyglutamine proteins (22). These results demonstrate that both GFP-degron and GFP-Δ9CAT exhibit decreased solubility and aggregation, induce and transiently associate with the chaperone Hsp70, and establish GFP-degron and GFP-Δ9CAT as *bona fide* misfolded proteins.

### Misfolded proteins undergo proteasomal degradation

Both Link *et al.* (18) and our group observed GFP-degron as perinuclear aggregates (Fig. 1), though GFP-degron$^+$ cells were always only a modest fraction (5–15%) of the total cell population. Hence, we tested whether a proteolytic degradation of misfolded proteins occurred. Using the proteasome inhibitor MG-132, we detected an increased level of both GFP-degron and GFP-Δ9CAT by flow cytometry. MG-132, at a concentration as low as 2 μM (a concentration without severe cytotoxicity), induced a significant increase in GFP-degron$^+$ and GFP-Δ9CAT$^+$ cells, approaching the ratio of GFP$^+$ and GFP-wtCAT$^+$ cells (Fig. 2*A*). It is important to note that neither GFP-degron nor GFP-Δ9CAT was detected in soluble forms, and proteasome inhibition did not significantly change the appearance and topology of aggregates examined by fluorescent microscopy, which suggests that aggregation is a direct consequence of the presence of misfolded, undegradable ensembles. We found that 3-methyladenine, a specific inhibitor of autophagy, did not increase GFP-fluorescence (data not shown), suggesting that the stabilization observed with MG-132 was not due to an unspecific inhibition of the cellular proteolytic capacity. Altogether, these results define the proteasome responsible for the degradation of these misfolded proteins.

Flow cytometric histograms of MG-132-treated cell populations show that proteasome inhibition stabilizes GFP-degron and GFP-Δ9CAT at fluorescence intensities exceeding $10^2$ and $3 \times 10^2$, respectively, suggesting that misfolded species are tolerated below these tresholds (Fig. 2*B*). We determined the corresponding expression levels by densitometry of anti-GFP Western blots of total cell lysates (Fig. 2*C, D*). While traces of misfolded proteins were detected using these settings, inhibition of their turnover increased the average expression of GFP-degron and GFP-Δ9CAT to 2.2 *vs.* 0.9% of total cellular protein, respectively. These results are consistent with the higher peak of GFP-degron observed in flow cytometry (Fig. 2*B*). Considering the logarithmic scale of fluorescence and the abovementioned thresholds, we assume that maximal expression levels cannot exceed 1–2% of total cellular proteins, and that misfolded proteins in the range of ~0.02–0.04% of total cellular proteins are efficiently sensed and disposed.

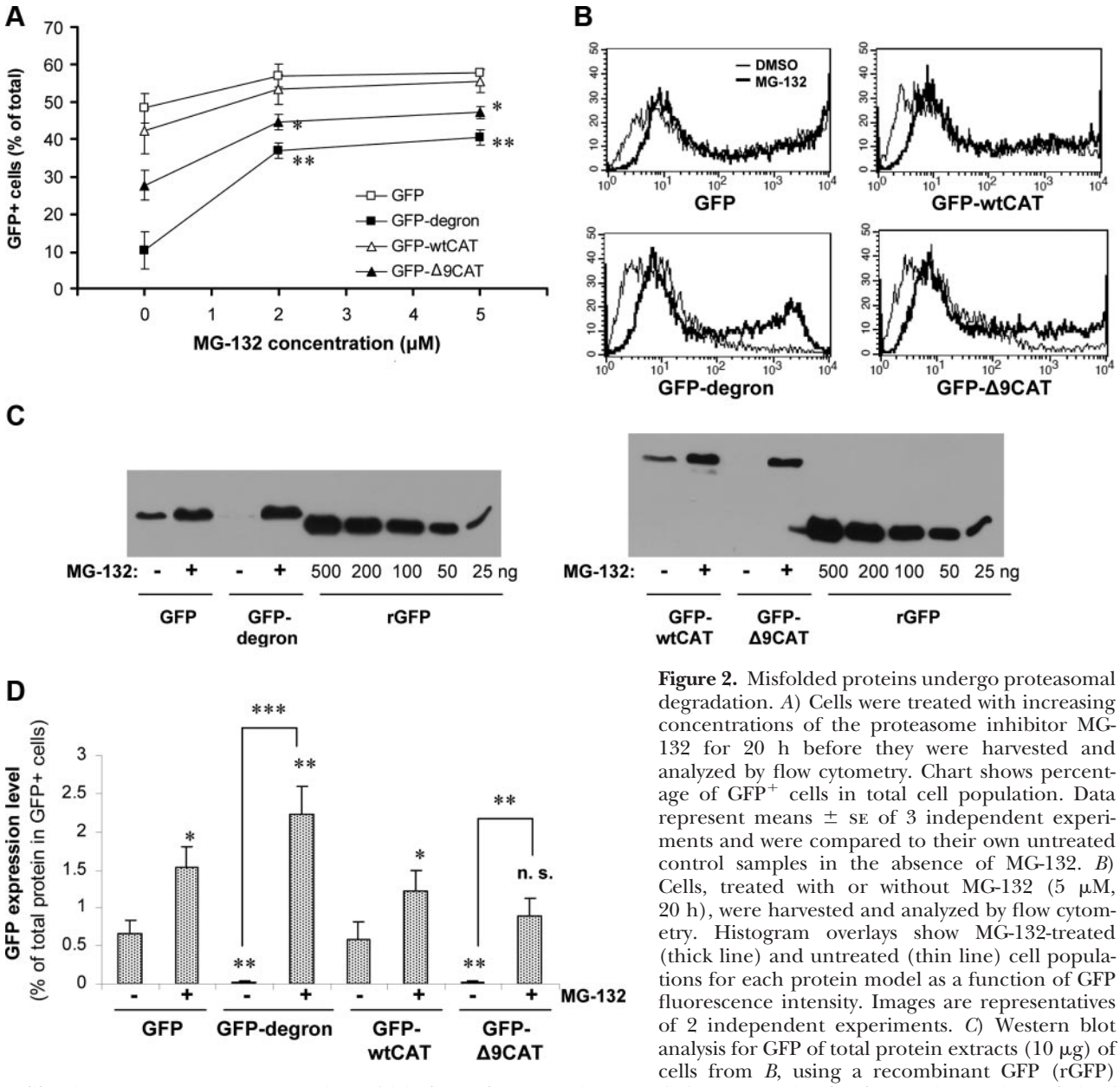


**Figure 2.** Misfolded proteins undergo proteasomal degradation. *A*) Cells were treated with increasing concentrations of the proteasome inhibitor MG-132 for 20 h before they were harvested and analyzed by flow cytometry. Chart shows percentage of $GFP^+$ cells in total cell population. Data represent means ± SE of 3 independent experiments and were compared to their own untreated control samples in the absence of MG-132. *B*) Cells, treated with or without MG-132 (5 μM, 20 h), were harvested and analyzed by flow cytometry. Histogram overlays show MG-132-treated (thick line) and untreated (thin line) cell populations for each protein model as a function of GFP fluorescence intensity. Images are representatives of 2 independent experiments. *C*) Western blot analysis for GFP of total protein extracts (10 μg) of cells from *B*, using a recombinant GFP (rGFP) calibration. Images are representatives of 2 independent experiments. *D*) GFP expression levels. Densitometric analysis of Western blots from *C*, normalized to their corresponding GFP positivities. Data represent means ± SE of 2 independent experiments and were compared to untreated GFP and GFP-wtCAT controls (asterisks on columns) and to GFP-degron/GFP-Δ9CAT in the absence or presence of MG-132, respectively (linked bars). n.s., not significant. $*P < 0.05$; $**P < 0.01$; $***P < 0.001$.

### Misfolded proteins activate the *hsp70* promoter

Since we could see an accumulation of Hsp70 protein with both misfolded proteins, we were interested whether they would induce transactivation of heat-shock factor 1 (HSF1), responsible for the induction of *hsp* genes. To accomplish this, we used a reporter construct harboring the *hsp70* promoter fused to firefly luciferase (23). GFP-degron expression resulted in a moderate induction of the reporter at 37°C by up to 4-fold compared to that of GFP (**Fig. 3*A***). GFP-Δ9CAT was able to induce the reporter gene at a smaller, comparable extent (3-fold increase compared to the induction by GFP-wtCAT). Induction of the reporter by misfolded proteins was completely blunted by cotransfection with HSF1 siRNA, confirming that the induction was entirely HSF1-dependent, consistent with previous results (data not shown; ref. 24). GFP-degron and GFP-Δ9CAT did not activate the endoplasmic reticulum chaperone, *grp78* promoter (data not shown), suggesting that misfolding of cytosolic proteins does not result in the activation of the endoplasmic reticulum unfolded protein response, consistent with recent studies in yeast (25–26).

We next addressed how misfolded proteins would interfere with the induction of the heat-shock response by a moderate proteotoxic heat stress (43°C). The presence of GFP-degron and GFP-Δ9CAT, neither

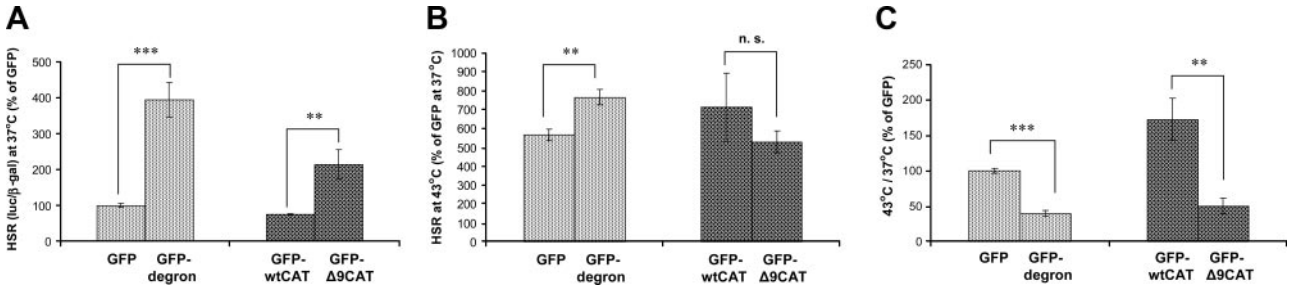


**Figure 3.** Misfolded proteins activate the *hsp70* promoter. HSF1-transactivation at 37°C (*A*), heat-induced HSF1-transactivation (*B*), and the ratio of induced and basal outputs (*C*). *A*, *B*) Along with the indicated constructs, cells were cotransfected with hsp70.1pr-luc and β-galactosidase (β-gal) plasmids. A second set (*B*) was given a heat shock at 43°C for 30 min. Luciferase and β-gal assays were performed 18 h later, and their ratios were expressed as percentages of the value obtained in the GFP sample. *C*) Alternatively, fold inductions in the heat-shock response were calculated by dividing the normalized (luc/β-gal) heat-shocked (43°C) values by their corresponding basal (37°C) values and are displayed in the chart as a percentage of the value obtained in the GFP sample. Data represent means ± SE of 7 independent experiments for GFP and GFP-degron and 3 independent experiments for GFP-wtCAT and GFP-Δ9CAT, respectively. Values were compared to the respective wild-type controls. n.s., not significant. $^{**}P < 0.01$; $^{***}P < 0.001$.

failed to synergize with nor compromised the heat-induced activity of the reporter gene construct, respectively, suggesting that the induction of the heat-shock response was not significantly changed by a transient expression of a single misfolded protein (Fig. 3*B*). However, misfolded proteins led to a higher basal level as well as a reduced reserve capacity of the heat-shock response, suggesting that the induction of heat-shock proteins was under a constant strain at basal conditions (Fig. 3*C*). We observed the same phenomenon with bovine serum albumin misdirected to the cytosol (GFP-cBSA) and with the coiled-coil region of the Golgi complex protein 170 fused to GFP (GFP170*), a nonpolyQ protein reported to form nuclear aggregates and colocalize with Hsp70, consistent with a previous reports (refs. 9, 24 and data not shown). Hence, we conclude that a transient expression of a single misfolded protein induces HSF1-dependent transactivation without a severe compromise of heat inducibility along with a reduced reserve capacity of the heat-shock response.

### Opposing effects by GFP-degron and GFP-Δ9CAT on chaperone-mediated folding

Chronic expression of polyQ proteins was previously shown to interfere with protein folding in *C. elegans* (17). To test this possibility in replicative cells, we asked how acute expression misfolded proteins would affect the activity of firefly luciferase, a metastable multidomain protein commonly used as a model substrate to monitor chaperone activity/function (27). Overexpression of GFP-degron caused a 25% decrease of luciferase activity compared to that of wild-type GFP-cotransfected cells at 37°C (**Fig. 4*A***). Surprisingly, GFP-Δ9CAT enhanced luciferase activity by 20% compared to that of GFP-wtCAT at 37°C (Fig. 4*B*). With increasing periods of time at 42°C heat shock, the difference between luciferase activities of both GFP *vs.* GFP-degron and GFP-wtCAT *vs.* GFP-Δ9CAT pairs disappeared. Similar phenomena were observed with MG-132, consistent with the proteasomal clearance of an extensive amount of mistranslated-misfolded proteins already at nonstress conditions (28). Hsp70 overexpression promoted luciferase folding by ~25% for all constructs even in the presence of MG-132 (data not shown), establishing that global manipulations of the proteostatic buffer were efficiently monitored by firefly luciferase. None of the interventions affected the activity of β-galactosidase (data not shown). We conclude that in contrast to global proteotoxic stresses (heat shock and MG-132), short-term expression of single misfolded proteins exerts a modest effect on chaperone-mediated protein folding.

### Misfolded proteins inhibit cell proliferation

We next investigated the consequences of protein misfolding on cell growth. Incorporation of the thymidine analog bromodeoxyuridine (BrdU) into genomic DNA is an indicator of cell division. To analyze rates of BrdU uptake in transfected and untransfected subpopulations we immunostained the cells with both anti-GFP and anti-BrdU antibodies. Image analyses of dual immunofluorescence data revealed that both GFP-degron$^+$ and GFP-Δ9CAT$^+$ cells incorporated less BrdU than their wild-type counterparts (**Fig. 5**). Induction of cell proliferation arrest was more pronounced with GFP-degron, suggesting a stronger effect of GFP-degron on cell growth. MG-132 (2 μM, 20 h) treatment completely blocked BrdU uptake (data not shown). Thus, similarly to proteasome inhibition, misfolded proteins arrest cell proliferation.

### Misfolded proteins promote stress-induced cell death

Although misfolded proteins inhibited cell proliferation (Fig. 5*B*), we detected neither any necrosis by propidium iodide exclusion nor apoptosis by sub-$G_1$ peak of DNA (data not shown). However, treatment of transfected cells with MG-132 resulted in an altered histogram with a distorted sub-$G_1$ peak containing cell

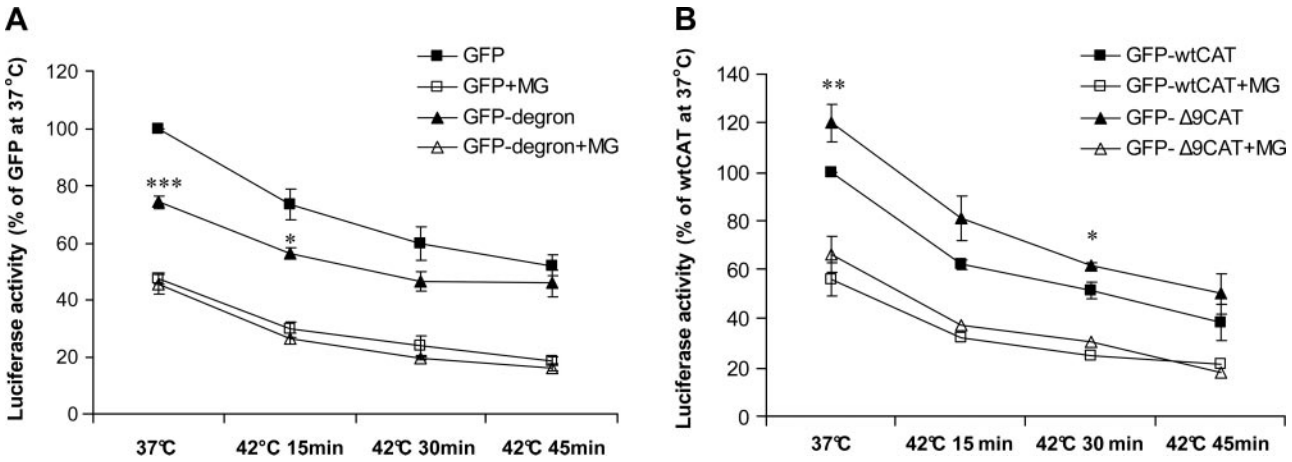


**Figure 4.** Opposing effects by GFP-degron and GFP-Δ9CAT on chaperone-mediated folding. GFP-degron compromises (*A*), while GFP-Δ9CAT enhances (*B*) firefly luciferase folding at 37°C. Along with the indicated protein models, cells were cotransfected with TK-luc and β-gal plasmids. After treatment with or without MG-132 (2 μM, 20 h), cells were either incubated at 37°C or given a heat shock at 42°C for the indicated periods of time. Immediately after the heat shock, cells were cooled on ice, lysed, and analyzed, as described in Materials and Methods. Charts show normalized luciferase (luc/β-gal) activities as a percentage of the value obtained in the respective wild-type controls at 37°C without MG-132 treatment. Data represent means ± SE of 3 independent experiments and were compared to the respective wild-type controls subjected to the same treatment. $*P < 0.05$; $**P < 0.01$; $***P < 0.001$.

debris along with a marked decrease in the number of intact cells (**Fig. 6*A***). Therefore, as a more appropriate marker of the number of intact (live) cells, a joint measure of cell proliferation and death, we calculated the area below the $G_1$-S-$G_2$/M peaks of $GFP^+$ cells (labeled by peaks in Fig. 6*A*). GFP-degron and GFP-Δ9CAT transfection combined with MG-132 treatment resulted in a lesser amount of intact $GFP^+$ cells compared to their wild-type controls already at 37°C (Fig. 6*B*). Notably, there was a further sharp decrease in the number of GFP-degron- or GFP-Δ9CAT-transfected intact cells when they were given a moderate heat shock (43°C, 30 min) that did not affect GFP and GFP-wtCAT controls.

To obtain an independent measure of cell death, we performed annexin staining, detecting cell death from early apoptosis through late necrosis. $GFP^+$ cells displayed enhanced annexin staining compared with GFP-negative population and MG-132 treatment resulted in

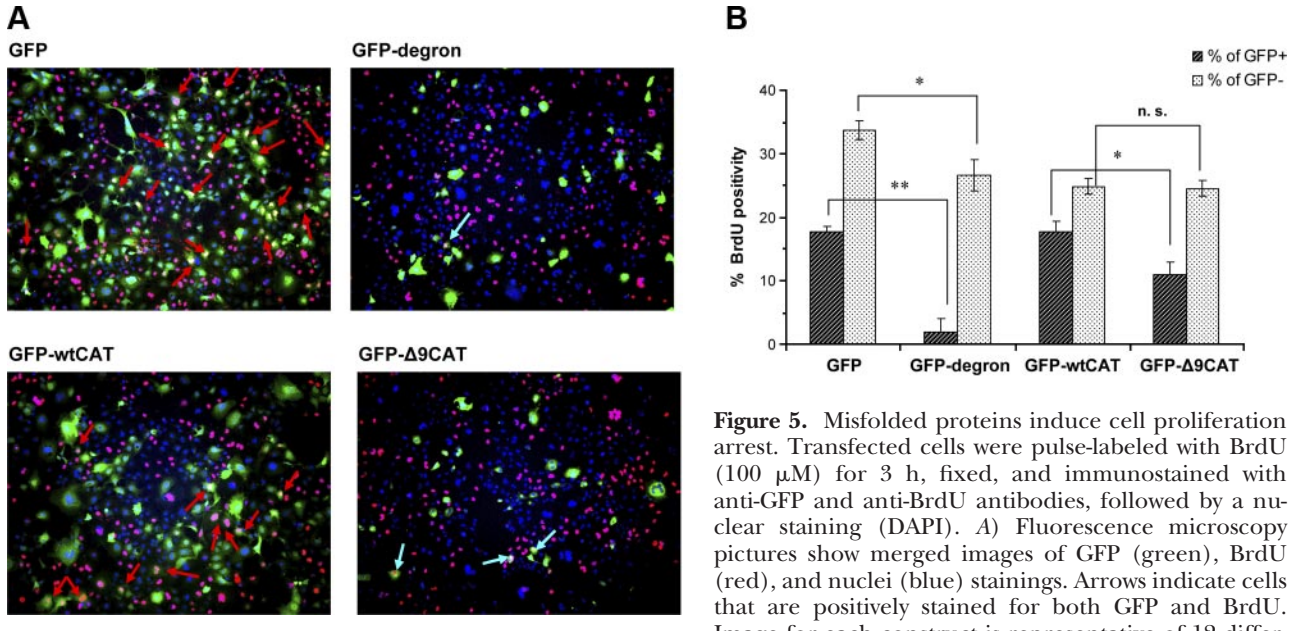


**Figure 5.** Misfolded proteins induce cell proliferation arrest. Transfected cells were pulse-labeled with BrdU (100 μM) for 3 h, fixed, and immunostained with anti-GFP and anti-BrdU antibodies, followed by a nuclear staining (DAPI). *A*) Fluorescence microscopy pictures show merged images of GFP (green), BrdU (red), and nuclei (blue) stainings. Arrows indicate cells that are positively stained for both GFP and BrdU. Image for each construct is representative of 12 different regions from 2 independent experiments. *B*) Quantification of dual immunofluorescence data. Six different areas randomly selected from each protein model with an average of 600–700 cells/area were first counted for single DAPI, GFP, and BrdU signals. Double positives for both GFP and BrdU signals were then counted, and calculations were done accordingly to determine percentages of BrdU positivity in $GFP^+$ (dark bars) and GFP-negative (light bars) subpopulations. Data represent means ± SE of 2 independent experiments and were compared to the respective wild-type controls. n.s., not significant. $*P < 0.05$; $**P < 0.01$.

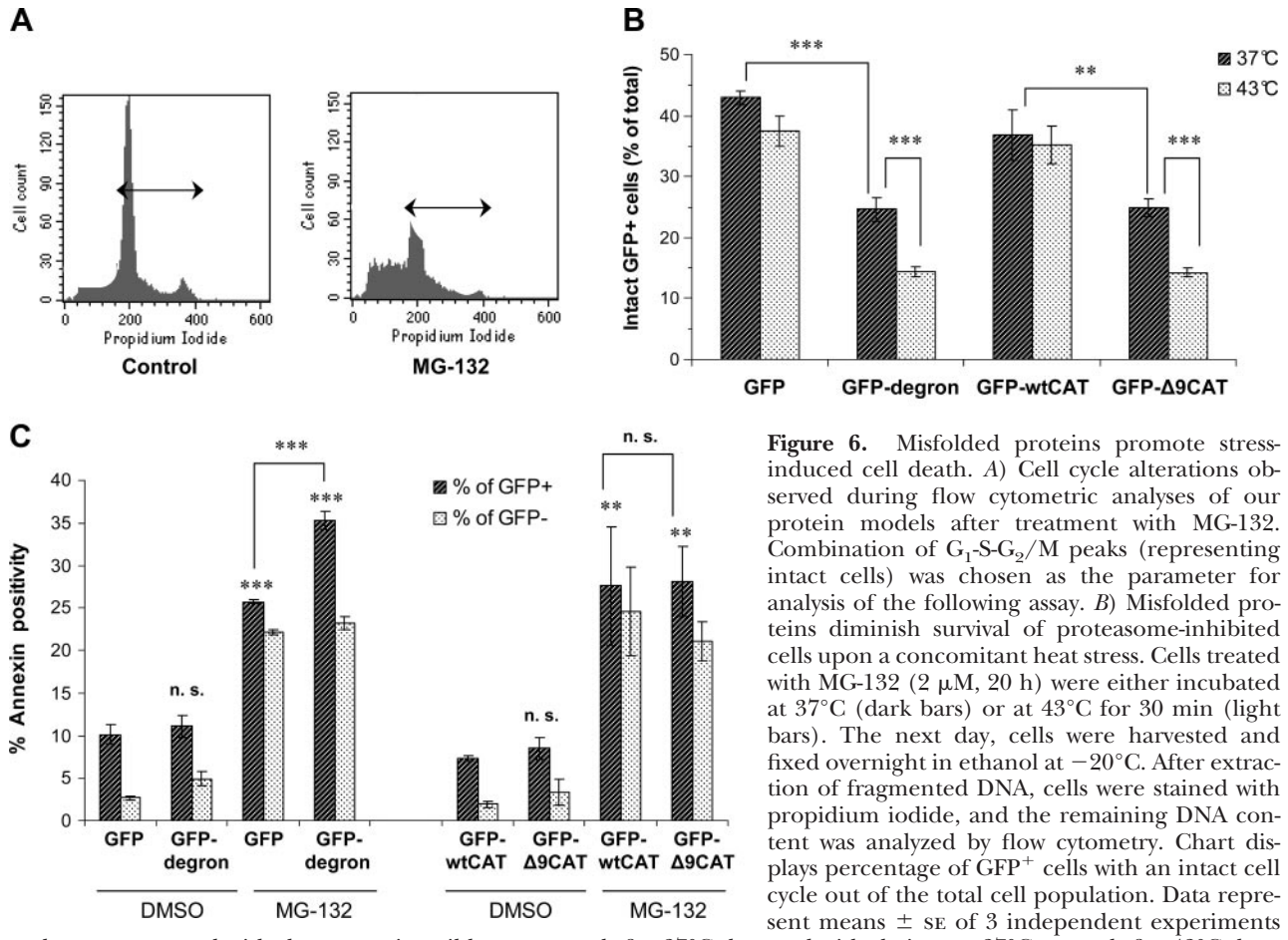


**Figure 6.** Misfolded proteins promote stress-induced cell death. *A*) Cell cycle alterations observed during flow cytometric analyses of our protein models after treatment with MG-132. Combination of $G_1$-S-$G_2$/M peaks (representing intact cells) was chosen as the parameter for analysis of the following assay. *B*) Misfolded proteins diminish survival of proteasome-inhibited cells upon a concomitant heat stress. Cells treated with MG-132 (2 μM, 20 h) were either incubated at 37°C (dark bars) or at 43°C for 30 min (light bars). The next day, cells were harvested and fixed overnight in ethanol at −20°C. After extraction of fragmented DNA, cells were stained with propidium iodide, and the remaining DNA content was analyzed by flow cytometry. Chart displays percentage of $GFP^+$ cells with an intact cell cycle out of the total cell population. Data represent means ± SE of 3 independent experiments and were compared with the respective wild-type controls for 37°C data and with their own 37°C controls for 43°C data. *C*) Misfolded GFP-degron, but not GFP-Δ9CAT, induces annexin positivity upon proteasome inhibition. Cells treated with or without MG-132 (2 μM, 42 h) were stained with annexin V, and analyzed by flow cytometry. The chart shows the percentage of annexin positivity in $GFP^+$ (dark bars) and GFP-negative (light bars) subpopulations for each protein model. Data represent means ± SE of 3 independent experiments, and $GFP^+$ values were compared to GFP and GFP-wtCAT controls (asterisks on columns) and GFP-degron/GFP-Δ9CAT to their respective MG-132-treated wild-type control (linked bars). n.s., not significant. $^{**}P < 0.01$; $^{***}P < 0.001$.

an increase in annexin-positivity from 10 to 25%, consistent with a general proteotoxicity induced by proteasome inhibition (Fig. 6*C*). Similarly to the previous propidium iodide data, there was no significant difference between annexin staining of GFP-degron- and GFP-Δ9CAT-transfected cells compared to that of their wild-type counterparts. However, MG-132 treatment of cells expressing GFP-degron, but not GFP-Δ9CAT, yielded a significantly higher annexin positivity compared to controls (Fig. 6*C*). These results confirm the GFP-degron-related findings presented in Fig. 6*B* and suggest that some form of GFP-Δ9CAT-induced cell death may escape detection by annexin in our experimental conditions. Nevertheless, when GFP-Δ9CAT cells underwent a moderate heat shock, they also displayed an increased annexin positivity comparable to that of GFP-degron (data not shown). Moreover, we obtained similar results with 2 other misfolded protein models, GFP-cBSA and GFP170*, upon MG-132 treatment (Supplemental Fig. S2). Thus, diverse misfolded proteins sensitize cells to manifest enhanced cytotoxicity in response to stress.

### HSF1, Hsp70, and SIRT1 protect from GFP-degron-induced cytotoxicity

We next addressed how genetic activation of stress-responsive mechanisms would combat the cytotoxicity induced by GFP-degron. HSF1 and Hsp70 are important determinants of the heat-shock response, ameliorating toxicity of neurodegenerative models (10, 29–30). SIRT1 is an $NAD^+$-dependent protein deacetylase, which was reported to control HSF1 activity by prolonging its DNA binding through deacetylation (31). It was also shown to be protective in initial studies against polyglutamine-induced cytotoxicity in both *C. elegans* and mammalian neurons (32), though its general role in invertebrate longevity has been questioned (33). SIRT6 is a nuclear sirtuin paralog implicated in dietary restriction and the metabolic syndrome; however, there are no data on its role in proteostasis (34).

All the HSF1, Hsp70, SIRT1, and SIRT6 constructs were strongly overexpressed upon transfection (**Fig. 7*A***). None of the constructs caused any significant difference in the number of GFP-degron$^+$ cells (*i.e.*,

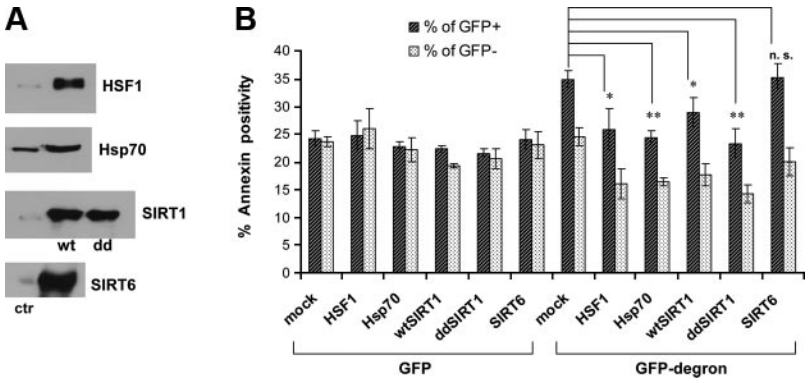


**Figure 7.** HSF1, Hsp70, and SIRT1 protect from GFP-degron-induced cytotoxicity. *A*) HSF1, Hsp70, SIRT1s, and SIRT6 are strongly overexpressed on transfection. Cells were transfected with mock (ctr), HSF1, Hsp70, wtSIRT1, deacetylase-deficient H363Y mutant SIRT1 (ddSIRT1), and SIRT6 constructs, respectively, for 24 h, lysed, and analyzed by Western blotting for the respective proteins. Images are representatives of 2 independent experiments. *B*) Cell death of MG-132-treated (2 μM, 42 h) cells. Cotransfections of the constructs were done at a ratio of 1:1 (misfolded protein construct:modulator). Annexin assay was performed as described in Materials and Methods. Chart shows the percentage of annexin positivity in $GFP^+$ (dark bars) and GFP-negative (light bars) subpopulations for each cotransfection. Renilla luciferase plasmid served as mock. Data represent means ± SE of 3 independent experiments. Statistical comparisons were made between the respective $GFP^+$ samples compared to mock-cotransfected sample. n.s., not significant. $*P < 0.05$; $**P < 0.01$.

cells expressing and not degrading GFP-degron) in the absence or presence of MG-132 (data not shown), suggesting they did not alter the turnover of GFP-degron. HSF1, Hsp70, and SIRT1 constructs were all found to prevent cell death in MG-132-treated GFP-degron-expressing cells (Fig. 7*B*). Interestingly, SIRT1-mediated recovery from GFP-degron-induced cytotoxicity was independent of the deacetylase activity of SIRT1, as both wild-type (wtSIRT1) and the deacetylase-deficient H363Y mutant (ddSIRT1) were protective. In contrast, SIRT6 did not exert a protective effect, giving an independent evidence for the specific action of SIRT1. This finding is in line with a recent study where SIRT1-induced neuroprotection was found to be independent of its deacetylase activity (35), suggesting a novel, noncatalytic mechanism of cytoprotection for SIRT1.

## DISCUSSION

Conformational diseases share common features: the accumulation of non-native protein species and a consequent cytotoxicity. Here we have isolated the general effects elicited by single misfolded polypeptides by expressing 2 *bona fide* misfolded proteins not occurring in the mammalian cytosol. Both GFP-fused degron and C-terminally truncated chloramphenicol acetyltransferase lost solubility and exhibited aggregation, transiently associated with and induced the expression of the chaperone Hsp70, underwent a proteasomal degradation in the majority of cells, induced growth arrest, and caused cytotoxicity in response to stress, which was ameliorated by stress-responsive mechanisms (**Fig. 8**). These features obtained with diverse misfolded proteins are consistent with an inherent toxicity of the misfolded ensembles *per se*.

Loss of a stabilizing interaction mediated by a C-terminal residue in Δ9CAT disrupts its stability and results in inclusion body formation in *E. coli* (19, 36). Our results indicate that GFP-Δ9CAT instability also induces its misfolding in mammalian cells (Figs. 1 and 2, and Supplemental Fig. S1). The 16-residue degron peptide supplements proteins with a C-terminal amphipathic α helix conferring destabilization to the extended proteins (18, 37). GFP-degron appears to be a Janus-faced molecule, *i.e.*, both an *in vivo* ubiquitin-proteasome system (UPS) reporter (6, 38) and a misfolded protein (Fig. 1 and ref. 18). This dual behavior can be explained by considering a primary misfolding of GFP-degron and its chaperone-mediated disposal by the UPS (Fig. 8 and ref. 18), a pathway identical to that of global protein misfolding (13). This model is supported by the similar phenotype (exhibiting aggregation, chaperone induction, growth inhibition) of GFP-degron to several misfolded proteins: YFP point mutants in yeast (26), GFP170* (present study and ref. 9), and GFP-Δ9CAT (present study), respectively. In addition, yeast Ura3p fused to degron requires the Hsp70/Hsp40 orthologs Ssa1p/Ydj1p for both its proteasomal degradation and solubility (39), in agreement with a degron-induced misfolding of Ura3p.

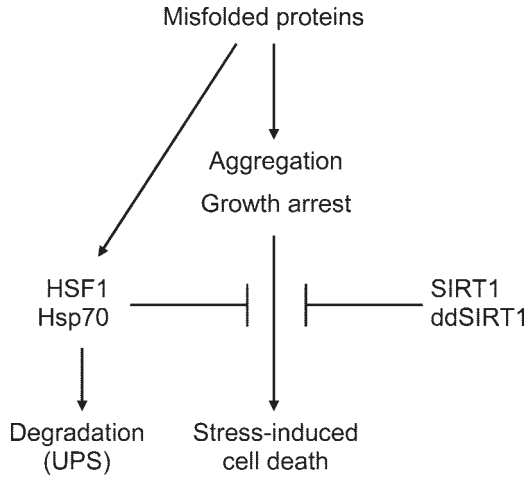


**Figure 8.** Misfolded proteins in mammalian cells. Misfolded proteins induce the heat-shock response and are turned over by the UPS in the majority of cells. In cells that are incompetent to degrade them, they form aggregates and cause growth arrest. Upon various stresses, such as the inhibition of UPS or heat shock, misfolded proteins promote cell death. The genetic up-regulation of the heat-shock response (HSF1 or Hsp70) and the sirtuin SIRT1, independently of its deacetylase activity (ddSIRT1), protects from stress-induced cytotoxicity.

Our findings suggest that aggregate formation prevails if the level of misfolded proteins exceeds the proteostatic capacity of the cell. Upon transient transfection in our study (Fig. 1*B*) and in that of Link *et al.* (18) misfolded proteins were efficiently cleared from the majority of cell population and formed aggregates in $GFP^+$ cells. These effects were augmented by proteasome inhibition (Fig. 2). Overexpression of Hsp70 or HSF1 did not decrease the number of GFP-degron$^+$ cells (*i.e.*, did not increase the turnover of the protein), which, along with the yeast study on Ura3p-degron (39), suggests that chaperones are required for but do not limit GFP-degron degradation. These findings suggest that the UPS is a rate-limiting step in the chaperone-mediated disposal of misfolded proteins and offer a rationale for GFP-degron as an *in vivo* marker measuring UPS capacity.

The roles of Hsp70 and HSF1 in cells expressing misfolded proteins (Fig. 7) corroborate the well-documented role of the heat-shock response in the recognition and defense against proteotoxicity (22, 40). The decreasing order of intensity of Hsp70 induction by GFP-degron > GFP-Δ9CAT > GFP-cBSA = GFP170* indicates a proportional release of HSF1 from its repressing chaperone complex in response to misfolding. This effect is consistent with the previously reported, dose-dependent effect of cytosolic BSA on HSF1 activation (24). Considering the ~1–2% maximal level of misfolded proteins induced by proteasome inhibition and an induction of Hsp70 in the heat-shock range, we speculate that misfolded ensembles at the 0.02–0.04% threshold level may elicit a signal potent enough to provoke a significant threat, namely, cell cycle arrest. This threat, however, appears to be compensated in our experimental conditions by a highly efficient recognition/disposal (demonstrated by the negligible effects of misfolded protein expression on thermotolerance and on cytotoxicity). Recent studies demonstrate a specific, HSF1-mediated cytosolic unfolded protein response within the wider heat-shock response/proteostatic network in yeast and plants (25–26, 41–42). Our results, by showing a selective activation of hsp70 *vs.* the ER stress marker grp78 promoter (Fig. 3*A* and data not shown), extend the existence of this specific cytosolic response to mammalian cells. The misfolded proteins used in this study provide a tractable model to identify the cytosolic unfolded protein response at the systems level in mammalian cells.

We observed a differential, but modest, effect of GFP-degron and GFP-Δ9CAT on firefly luciferase folding (Fig. 4). The reason for this difference is unknown. It may be that GFP-degron and GFP-Δ9CAT differentially affect protein transcription/translation. Though we did not test luciferase mRNA and protein levels, the similar β-galactosidase activities and the equal residual activities after heat shock or MG-132 treatment exclude such a possibility. The GFP-Δ9CAT-induced luciferase activation may be explained by its less pronounced effects (*i.e.*, higher ratio of $GFP^+$ cells, slower turnover, smaller *hsp70*-promoter induction, and decreased inhibition of cell proliferation), suggesting less toxic misfolded species formed by GFP-Δ9CAT, which in turn may activate chaperone-mediated folding. Though these data do not allow a clear conclusion, the modest effects and the clear dissection from toxicity (Figs. 5 and 6) suggest chaperone-mediated folding is not the major determinant of short-term action of individual misfolded proteins.

Our results in COS-7 cells recapitulate the proliferation arrest obtained with single misfolded mutants, including polyQ103-GFP in HEK-293 cells (6), GFP170* in COS-7 cells (9), YFP mutants (26), and azetidine-carboxylate in yeast (43), which suggests a conserved, general effect of protein misfolding. This occurs in $GFP^+$ cells (*i.e.*, cells that are unable to degrade the misfolded proteins; Fig. 8). The almost complete loss of BrdU incorporation may be consistent with a $G_1$ arrest. As in COS-7 cells, the SV40 large T-antigen inactivates both Rb and p53; it is tempting to speculate that mechanisms distinct from these checkpoint responses may inhibit proliferation. Indeed, such mechanisms arising from the inherent toxicity of misfolding have been demonstrated, such as sequestration of the growth-promoting CBP into aggregates (5, 9). Alternatively, growth inhibition may be due to the adaptive response, *e.g.*, HSF1 mediating reversible cell cycle arrest in yeast (43) or increased Hsp70 inhibiting growth (44–45). Though the molecular pathways induced by misfolded proteins remain to be analyzed, our findings on transformed cells might have a potential effect in nontransformed mitotic cells or stem cells.

A number of studies demonstrated extensive apoptosis using disease-associated mutants in cell (mostly neuronal) culture and in animal models (1, 7). However, we have not been able to detect death of immortalized COS-7 cells expressing misfolded proteins in nonstress conditions during the time scale of our experiments. Whether the long-term expression of a single misfolded protein leads to cell loss requires further studies. We also consider the possibility that misfolded proteins may induce cytotoxicity in neurons, where proteostatic defenses, such as the heat-shock response, are inherently weaker (46–47). Moreover, paralysis in the absence of apoptosis in *C. elegans* muscle expressing GFP-degron (18) and proliferation arrest (our study) suggest that severe dysfunctionality does not necessarily need cell death. The augmentation of death observed upon proteasome inhibition or heat shock by 4 misfolded mutants (Fig. 6 and Supplemental Fig. S2) indicates that already a short-term expression of misfolded ensembles compromise cells to mount an efficient adaptive response to proteotoxic stress. Defective stress tolerance seems to be a deleterious consequence of misfolding, as up-regulation of 2 stress-responsive mechanisms, the heat-shock response (HSF1 and Hsp70), as well as the sirtuin SIRT1, conferred protection (Fig. 7). Our findings extend earlier studies on the beneficial role of chaperones in various models (18, 40). The cytoprotective effect by chaperones may either lie in the restoration of protein homeostasis and/or the negative regulation by Hsp70 of death signals *via* p38 and JNK (48–49).

Our findings on the SIRT1 overexpression protecting

from GFP-degron-induced proteotoxicity confirm previous results involving neurodegenerative models (32, 50–51). Moreover, the lack of effect of SIRT6 overexpression indicates divergent roles for sirtuin paralogs in mammals. SIRT1-dependent deacetylation of key signaling molecules including HSF1 and consequent cellular events have been extensively reported (31, 52). However, our study did not demonstrate a requirement of deacetylase activity, suggesting the SIRT1-mediated response did not demand an increased deacetylation/activation of HSF1 in our model (Fig. 7*B*). Recently, growing body of evidence shows deacetylase-independent functions of SIRT1 (53–55) including neuroprotection (35); however, the molecular mechanism of SIRT1 remains enigmatic. Our results extend these functions to protein misfolding and recall tests on the involvement of SIRT1 deacetylase activity in protection from neurodegenerative disease models (32, 50–51). Finding the proper role for SIRT1 is especially important in the light of our recent demonstration of the inability of SIRT1 orthologs to extend life span in invertebrates (33), which has implications on the development and use of SIRT1 activators as potential drug candidates (56).

Our results show that the action of misfolded proteins depends on the proteostatic balance and cellular heterogeneity. Protein misfolding is not limited to single genes/proteins, but it rather involves a significant fraction of the proteome probably due to destabilizing SNPs (57), mistranslation (2, 28, 58), and post-translational modifications. We note that the level of misfolded proteins in our study is comparable to protein carbonyls in aged tissues (3–4). Lack of dilution of damage as well as the age-associated collapse and/or intrinsic weakness of proteostasis precipitate symptoms particularly in postmitotic neurons during aging (16, 46–47). Our findings raise a question whether protein misfolding would induce damage to the replicative compartment *in situ*, which may have implications for aging of regenerating tissues. Indeed, dystrophy of hair follicles has been reported in a mistranslation mouse model (2). Detrimental outcome of misfolding may also shape the evolution of tumors, where intensive growth (translation) and high stress are associated with the absolute reliance on HSF1 (59). These hypotheses, as well as the long-term effects of misfolded proteins on cellular fitness, are subjects of future studies. As a conclusion, our study provides a mammalian cellular model of misfolded proteins and reveals that short-term expression of single misfolded proteins independently of sequence and function inhibit proliferation and stress adaptation in replicating cells. FJ

The authors thank Kerstin Bellman (Heinrich-Heine University, Düsseldorf, Germany), László Buday (Semmelweis University, Budapest, Hungary), Heim Cohen (Bar-Ilan University, Ramat-Gan, Israel), László Hunyady (Semmelweis University), Richard I. Morimoto (Northwestern University, Evanston, IL, USA), Lea Sistonen (Abo Akademi University, Turku, Finland), Elizabeth Sztul (University of Alabama, Birmingham, AL, USA), and Richard Voellmy (University of Miami, Miami, FL, USA) for generously sharing reagents. The authors are indebted to Gergely Imre, Ákos Putics, and Minh Tu Nguyen for experimental help, Beáta Gilányi for technical help, and the members of the Stress Group and the anonymous reviewers of this manuscript for helpful comments and suggestions. This work was supported by research grants from the EU (FP6-518230 PROTEOMAGE, FP7–200970 WhyWeAge, TÁMOP-4.2.2/B-10/1-2010-0013), from a joint grant of the Hungarian Science Foundation and Norway Grants (NNF-78794), and from the Hungarian Science Foundation (OTKA K69105 and OTKA-K83314). C.S. is a Bolyai Research Scholar of the Hungarian Academy of Sciences.

## REFERENCES

1. Soto, C. (2003) Unfolding the role of protein misfolding in neurodegenerative diseases. *Nat. Rev. Neurosci.* **4,** 49–60
2. Lee, J. W., Beebe, K., Nangle, L. A., Jang, J., Longo-Guess, C. M., Cook, S. A., Davisson, M. T., Sundberg, J. P., Schimmel, P., and Ackerman, S. L. (2006) Editing-defective tRNA synthetase causes protein misfolding and neurodegeneration. *Nature* **443,** 50–55
3. Dobson, C. M. (2003) Protein folding and misfolding. *Nature* **426,** 884–890
4. Stadtman, E. R., and Levine, R. L. (2003) Free radical-mediated oxidation of free amino acids and amino acid residues in proteins. *Amino Acids* **25,** 207–218
5. Nucifora, F. C., Jr., Sasaki, M., Peters, M. F., Huang, H., Cooper, J. K., Yamada, M., Takahashi, H., Tsuji, S., Troncoso, J., Dawson, V. L., Dawson, T. M., and Ross, C. A. (2001) Interference by huntingtin and atrophin-1 with cbp-mediated transcription leading to cellular toxicity. *Science* **291,** 2423–2428
6. Bence, N. F., Sampat, R. M., and Kopito, R. R. (2001) Impairment of the ubiquitin-proteasome system by protein aggregation. *Science* **292,** 1552–1555
7. Bucciantini, M., Giannoni, E., Chiti, F., Baroni, F., Formigli, L., Zurdo, J., Taddei, N., Ramponi, G., Dobson, C. M., and Stefani, M. (2002) Inherent toxicity of aggregates implies a common mechanism for protein misfolding diseases. *Nature* **416,** 507–511
8. Bucciantini, M., Calloni, G., Chiti, F., Formigli, L., Nosi, D., Dobson, C. M., and Stefani, M. (2004) Prefibrillar amyloid protein aggregates share common features of cytotoxicity. *J. Biol. Chem.* **279,** 31374–31382
9. Fu, L., Gao, Y. S., and Sztul, E. (2005) Transcriptional repression and cell death induced by nuclear aggregates of non-polyglutamine protein. *Neurobiol. Dis.* **20,** 656–665
10. Morimoto, R. I. (2008) Proteotoxic stress and inducible chaperone networks in neurodegenerative disease and aging. *Genes Dev.* **22,** 1427–1438
11. Ananthan, J., Goldberg, A. L., and Voellmy, R. (1986) Abnormal proteins serve as eukaryotic stress signals and trigger the activation of heat shock genes. *Science* **232,** 522–524
12. Voellmy, R., and Boellmann, F. (2007) Chaperone regulation of the heat shock protein response. *Adv. Exp. Med. Biol.* **594,** 89–99
13. Hartl, F. U., and Hayer-Hartl, M. (2002) Molecular chaperones in the cytosol: from nascent chain to folded protein. *Science* **295,** 1852–1858
14. Verbeke, P., Fonager, J., Clark, B. F., and Rattan, S. I. (2001) Heat shock response and ageing: mechanisms and applications. *Cell Biol. Int.* **25,** 845–857
15. Powers, E. T., Morimoto, R. I., Dillin, A., Kelly, J. W., and Balch, W. E. (2009) Biological and chemical approaches to diseases of proteostasis deficiency. *Annu. Rev. Biochem.* **78,** 959–991
16. Ben-Zvi, A., Miller, E. A., and Morimoto, R. I. (2009) Collapse of proteostasis represents an early molecular event in *Caenorhabditis elegans* aging. *Proc. Natl. Acad. Sci. U. S. A.* **106,** 14914–14919
17. Gidalevitz, T., Ben-Zvi, A., Ho, K. H., Brignull, H. R., and Morimoto, R. I. (2006) Progressive disruption of cellular protein folding in models of polyglutamine diseases. *Science* **311,** 1471–1474
18. Link, C. D., Fonte, V., Hiester, B., Yerg, J., Ferguson, J., Csontos, S., Silverman, M. A., and Stein, G. H. (2006) Conversion of green fluorescent protein into a toxic, aggregation-prone protein by C-terminal addition of a short peptide. *J. Biol. Chem.* **281,** 1808–1816
19. Robben, J., Van der Schueren, J., and Volckaert, G. (1993) Carboxyl terminus is essential for intracellular folding of chloramphenicol acetyltransferase. *J. Biol. Chem.* **268,** 24555–24558

20. Tamas, P., Solti, Z., Bauer, P., Illes, A., Sipeki, S., Bauer, A., Farago, A., Downward, J., and Buday, L. (2003) Mechanism of epidermal growth factor regulation of Vav2, a guanine nucleotide exchange factor for Rac. *J. Biol. Chem.* **278,** 5163–5171
21. Shaw, W. V. (1975) Chloramphenicol acetyltransferase from chloramphenicol-resistant bacteria. *Methods Enzymol.* **43,** 737–755
22. Kim, S., Nollen, E. A., Kitagawa, K., Bindokas, V. P., and Morimoto, R. I. (2002) Polyglutamine protein aggregates are dynamic. *Nat. Cell Biol.* **4,** 826–831
23. Westerheide, S. D., Bosman, J. D., Mbadugha, B. N., Kawahara, T. L., Matsumoto, G., Kim, S., Gu, W., Devlin, J. P., Silverman, R. B., and Morimoto, R. I. (2004) Celastrols as inducers of the heat shock response and cytoprotection. *J. Biol. Chem.* **279,** 56053–56060
24. Guo, Y., Guettouche, T., Fenna, M., Boellmann, F., Pratt, W. B., Toft, D. O., Smith, D. F., and Voellmy, R. (2001) Evidence for a mechanism of repression of heat shock factor 1 transcriptional activity by a multichaperone complex. *J. Biol. Chem.* **276,** 45791–45799
25. Metzger, M. B., and Michaelis, S. (2009) Analysis of quality control substrates in distinct cellular compartments reveals a unique role for Rpn4p in tolerating misfolded membrane proteins. *Mol. Biol. Cell* **20,** 1006–1019
26. Geiler-Samerotte, K. A., Dion, M. F., Budnik, B. A., Wang, S. M., Hartl, D. L., and Drummond, D. A. (2011) Misfolded proteins impose a dosage-dependent fitness cost and trigger a cytosolic unfolded protein response in yeast. *Proc. Natl. Acad. Sci. U. S. A.* **108,** 680–685
27. Michels, A. A., Kanon, B., Konings, A. W., Ohtsuka, K., Bensaude, O., and Kampinga, H. H. (1997) Hsp70 and Hsp40 chaperone activities in the cytoplasm and the nucleus of mammalian cells. *J. Biol. Chem.* **272,** 33283–33289
28. Schubert, U., Anton, L. C., Gibbs, J., Norbury, C. C., Yewdell, J. W., and Bennink, J. R. (2000) Rapid degradation of a large fraction of newly synthesized proteins by proteasomes. *Nature* **404,** 770–774
29. Warrick, J. M., Chan, H. Y., Gray-Board, G. L., Chai, Y., Paulson, H. L., and Bonini, N. M. (1999) Suppression of polyglutamine-mediated neurodegeneration in *Drosophila* by the molecular chaperone HSP70. *Nat. Genet.* **23,** 425–428
30. Auluck, P. K., Chan, H. Y., Trojanowski, J. Q., Lee, V. M., and Bonini, N. M. (2002) Chaperone suppression of alpha-synuclein toxicity in a *Drosophila* model for Parkinson's disease. *Science* **295,** 865–868
31. Westerheide, S. D., Anckar, J., Stevens, S. M., Jr., Sistonen, L., and Morimoto, R. I. (2009) Stress-inducible regulation of heat shock factor 1 by the deacetylase SIRT1. *Science* **323,** 1063–1066
32. Parker, J. A., Arango, M., Abderrahmane, S., Lambert, E., Tourette, C., Catoire, H., and Neri, C. (2005) Resveratrol rescues mutant polyglutamine cytotoxicity in nematode and mammalian neurons. *Nat. Genet.* **37,** 349–350
33. Burnett, C., Valentini, S., Cabreiro, F., Goss, M., Somogyvari, M., Piper, M. D., Hoddinott, M., Sutphin, G. L., Leko, V., McElwee, J. J., Vazquez-Manrique, R. P., Orfila, A. M., Ackerman, D., Au, C., Vinti, G., Riesen, M., Howard, K., Neri, C., Bedalov, A., Kaeberlein, M., Soti, C., Partridge, L., and Gems, D. (2011) Absence of effects of Sir2 overexpression on lifespan in *C. elegans* and *Drosophila*. *Nature* **477,** 482–485
34. Kanfi, Y., Peshti, V., Gil, R., Naiman, S., Nahum, L., Levin, E., Kronfeld-Schor, N., and Cohen, H. Y. (2010) SIRT6 protects against pathological damage caused by diet-induced obesity. *Aging Cell* **9,** 162–173
35. Pfister, J. A., Ma, C., Morrison, B. E., and D'Mello, S. R. (2008) Opposing effects of sirtuins on neuronal survival: SIRT1-mediated neuroprotection is independent of its deacetylase activity. *PLoS One* **3,** e4090
36. Van der Schueren, J., Robben, J., and Volckaert, G. (1998) Misfolding of chloramphenicol acetyltransferase due to carboxy-terminal truncation can be corrected by second-site mutations. *Protein Eng.* **11,** 1211–1217
37. Gilon, T., Chomsky, O., and Kulka, R. G. (2000) Degradation signals recognized by the Ubc6p-Ubc7p ubiquitin-conjugating enzyme pair. *Mol. Cell. Biol.* **20,** 7214–7219
38. Bett, J. S., Cook, C., Petrucelli, L., and Bates, G. P. (2009) The ubiquitin-proteasome reporter GFPu does not accumulate in neurons of the R6/2 transgenic mouse model of Huntington's disease. *PLoS One* **4,** e5128
39. Metzger, M. B., Maurer, M. J., Dancy, B. M., and Michaelis, S. (2008) Degradation of a cytosolic protein requires endoplasmic reticulum-associated degradation machinery. *J. Biol. Chem.* **283,** 32302–32316
40. Muchowski, P. J., and Wacker, J. L. (2005) Modulation of neurodegeneration by molecular chaperones. *Nat. Rev. Neurosci.* **6,** 11–22
41. Trotter, E. W., Kao, C. M., Berenfeld, L., Botstein, D., Petsko, G. A., and Gray, J. V. (2002) Misfolded proteins are competent to mediate a subset of the responses to heat shock in *Saccharomyces cerevisiae*. *J. Biol. Chem.* **277,** 44817–44825
42. Sugio, A., Dreos, R., Aparicio, F., and Maule, A. J. (2009) The cytosolic protein response as a subcomponent of the wider heat shock response in *Arabidopsis*. *Plant Cell* **21,** 642–654
43. Trotter, E. W., Berenfeld, L., Krause, S. A., Petsko, G. A., and Gray, J. V. (2001) Protein misfolding and temperature up-shift cause G1 arrest via a common mechanism dependent on heat shock factor in *Saccharomycescerevisiae*. *Proc. Natl. Acad. Sci. U. S. A.* **98,** 7313–7318
44. Feder, J. H., Rossi, J. M., Solomon, J., Solomon, N., and Lindquist, S. (1992) The consequences of expressing hsp70 in *Drosophila* cells at normal temperatures. *Genes Dev.* **6,** 1402–1413
45. Song, J., Takeda, M., and Morimoto, R. I. (2001) Bag1-Hsp70 mediates a physiological stress signalling pathway that regulates Raf-1/ERK and cell growth. *Nat. Cell Biol.* **3,** 276–282
46. Batulan, Z., Shinder, G. A., Minotti, S., He, B. P., Doroudchi, M. M., Nalbantoglu, J., Strong, M. J., and Durham, H. D. (2003) High threshold for induction of the stress response in motor neurons is associated with failure to activate HSF1. *J. Neurosci.* **23,** 5789–5798
47. Kern, A., Ackermann, B., Clement, A. M., Duerk, H., and Behl, C. (2010) HSF1-controlled and age-associated chaperone capacity in neurons and muscle cells of *C. elegans*. *PLoS One* **5,** e8568
48. Gabai, V. L., Meriin, A. B., Mosser, D. D., Caron, A. W., Rits, S., Shifrin, V. I., and Sherman, M. Y. (1997) Hsp70 prevents activation of stress kinases. A novel pathway of cellular thermotolerance. *J. Biol. Chem.* **272,** 18033–18037
49. Mosser, D. D., Caron, A. W., Bourget, L., Denis-Larose, C., and Massie, B. (1997) Role of the human heat shock protein hsp70 in protection against stress-induced apoptosis. *Mol. Cell. Biol.* **17,** 5317–5327
50. Kim, D., Nguyen, M. D., Dobbin, M. M., Fischer, A., Sananbenesi, F., Rodgers, J. T., Delalle, I., Baur, J. A., Sui, G., Armour, S. M., Puigserver, P., Sinclair, D. A., and Tsai, L. H. (2007) SIRT1 deacetylase protects against neurodegeneration in models for Alzheimer's disease and amyotrophic lateral sclerosis. *EMBO J.* **26,** 3169–3179
51. Albani, D., Polito, L., Batelli, S., De Mauro, S., Fracasso, C., Martelli, G., Colombo, L., Manzoni, C., Salmona, M., Caccia, S., Negro, A., and Forloni, G. (2009) The SIRT1 activator resveratrol protects SK-N-BE cells from oxidative stress and against toxicity caused by alpha-synuclein or amyloid-beta (1–42) peptide. *J. Neurochem.* **110,** 1445–1456
52. Brooks, C. L., and Gu, W. (2009) How does SIRT1 affect metabolism, senescence and cancer? *Nat. Rev. Cancer* **9,** 123–128
53. Ghosh, H. S., Spencer, J. V., Ng, B., McBurney, M. W., and Robbins, P. D. (2007) Sirt1 interacts with transducin-like enhancer of split-1 to inhibit nuclear factor kappaB-mediated transcription. *Biochem. J.* **408,** 105–111
54. Vaitiekunaite, R., Butkiewicz, D., Krzesniak, M., Przybylek, M., Gryc, A., Snietura, M., Benedyk, M., Harris, C. C., and Rusin, M. (2007) Expression and localization of Werner syndrome protein is modulated by SIRT1 and PML. *Mech. Ageing Dev.* **128,** 650–661
55. Campagna, M., Herranz, D., Garcia, M. A., Marcos-Villar, L., Gonzalez-Santamaria, J., Gallego, P., Gutierrez, S., Collado, M., Serrano, M., Esteban, M., and Rivas, C. (2011) SIRT1 stabilizes PML promoting its sumoylation. *Cell Death Differ.* **18,** 72–79
56. Lavu, S., Boss, O., Elliott, P. J., and Lambert, P. D. (2008) Sirtuins: novel therapeutic targets to treat age-associated diseases. *Nat. Rev. Drug Discov.* **7,** 841–853
57. Ng, P. C., and Henikoff, S. (2006) Predicting the effects of amino acid substitutions on protein function. *Annu. Rev. Genomics. Hum. Genet.* **7,** 61–80
58. Drummond, D. A., and Wilke, C. O. (2008) Mistranslation-induced protein misfolding as a dominant constraint on coding-sequence evolution. *Cell* **134,** 341–352
59. Dai, C., Whitesell, L., Rogers, A. B., and Lindquist, S. (2007) Heat-shock factor 1 is a powerful multifaceted modifier of carcinogenesis. *Cell* **130,** 1005–1018

*Received for publication May 11, 2011.*
*Accepted for publication October 20, 2011.*